

UNCLASSIFIED

AD NUMBER

ADB019652

LIMITATION CHANGES

TO:

Approved for public release; distribution is unlimited.

FROM:

Distribution authorized to U.S. Gov't. agencies only; Test and Evaluation; JUN 1977. Other requests shall be referred to Air Force Armament Lab., Eglin AFB, FL.

AUTHORITY

USADTC LTR 4 SEP 1980

THIS PAGE IS UNCLASSIFIED

DECLASSIFIED / UNCLASSIFIED

AEDC-TR-77-43

AFATL-TR-77-48

cy.2



AERODYNAMIC CHARACTERISTICS AND FIN LOADS OF A BANK-TO-TURN, AIR-TO-AIR MISSILE CONCEPT AT SUPERSONIC MACH NUMBERS (U)

VON KARMAN GAS DYNAMICS FACILITY
ARNOLD ENGINEERING DEVELOPMENT CENTER
AIR FORCE SYSTEMS COMMAND
ARNOLD AIR FORCE STATION, TENNESSEE 37389

May 1977

Final Report for Period 8 - 10 December 1976

DISTRIBUTION LIMITED TO U. S. GOVERNMENT AGENCIES ONLY;
CONTAINS INFORMATION ON TEST AND EVALUATION OF MILITARY
HARDWARE; June 1977. OTHER REQUESTS FOR THIS DOCUMENT
MUST BE REFERRED TO AFATL/DLMI, EGLIN AFB, FL 32542

Per AFATL/DLMI letter 23 June 1977

Classified by AFATL/DL; Subject to General Declassification
Schedule of Executive Order 11652; Automatically
Downgraded at Two-Year Intervals; Declassify on December
31, 1981.

NATIONAL SECURITY INFORMATION
Unauthorized disclosure subject to criminal sanctions.

Prepared for

AIR FORCE ARMAMENT LABORATORY (DLMA)
EGLIN AIR FORCE BASE, FLORIDA 32542

DECLASSIFIED / UNCLASSIFIED

NOTICES

When U. S. Government drawings specifications, or other data are used for any purpose other than a definitely related Government procurement operation, the Government thereby incurs no responsibility nor any obligation whatsoever, and the fact that the Government may have formulated, furnished, or in any way supplied the said drawings, specifications, or other data, is not to be regarded by implication or otherwise, or in any manner licensing the holder or any other person or corporation, or conveying any rights or permission to manufacture, use, or sell any patented invention that may in any way be related thereto.

Qualified users may obtain copies of this report from the Defense Documentation Center.

References to named commercial products in this report are not to be considered in any sense as an endorsement of the product by the United States Air Force or the Government.

Do not return this copy. When not needed, destroy in accordance with pertinent security regulations.

APPROVAL STATEMENT

This technical report has been reviewed and is approved for publication.

FOR THE COMMANDER

Chauncey D. Smith, Jr.

CHAUNCEY D. SMITH, JR.
Lt Colonel, USAF
Chief Air Force Test Director, VKF
Directorate of Test

Alan L. Devereaux

ALAN L. DEVEREAUX
Colonel, USAF
Director of Test

CONFIDENTIAL

REPORT DOCUMENTATION PAGE		READ INSTRUCTIONS BEFORE COMPLETING FORM
1 REPORT NUMBER AEDC-TR-77-43 AFATL-TR-77-48	2 GOVT ACCESSION NO.	3 RECIPIENT'S CATALOG NUMBER
4 TITLE (and Subtitle) AERODYNAMIC CHARACTERISTICS AND FIN LOADS OF A BANK-TO-TURN, AIR-TO-AIR MISSILE CONCEPT AT SUPERSONIC MACH NUMBERS		5 TYPE OF REPORT & PERIOD COVERED Final Report, 8 - 10 December 1976
		6 PERFORMING ORG. REPORT NUMBER
7 AUTHOR(s) D. H. Fikes, ARO, Inc.		8 CONTRACT OR GRANT NUMBER(s)
9 PERFORMING ORGANIZATION NAME AND ADDRESS Arnold Engineering Development Center (XO) Air Force Systems Command Arnold Air Force Station, TN 37355		10 PROGRAM ELEMENT, PROJECT, TASK AREA & WORK UNIT NUMBERS Program Element 62602F Project 2069 Task 01
11 CONTROLLING OFFICE NAME AND ADDRESS Air Force Armament Laboratory (DLMA) Eglin Air Force Base, FL 32542		12 REPORT DATE May 1977
		13 NUMBER OF PAGES 42
14 MONITORING AGENCY NAME & ADDRESS (if different from Controlling Office)		15 SECURITY CLASS. (of this report) CONFIDENTIAL
		15a DECLASSIFICATION DOWNGRADING SCHEDULE GDS
16 DISTRIBUTION STATEMENT (of this Report) Distribution limited to U.S. Government agencies only; this report contains information on test and evaluation of military hardware; May 1977; other requests for this document must be referred to Air Force Armament Laboratory (AFATL/DLMA), Eglin Air Force Base, FL 32542.		
17 DISTRIBUTION STATEMENT (of the abstract entered in Block 20, if different from Report)		
18 SUPPLEMENTARY NOTES		
19 KEY WORDS (Continue on reverse side if necessary and identify by block number) air to air missiles fin loading short range (distance) supersonic flow static stability control		
20 ABSTRACT (Continue on reverse side if necessary and identify by block number) Static stability, axial-force, and fin-loading data were obtained on a proposed maneuvering air-to-air missile at Mach numbers 1.5, 2.5, and 3.5 with various combinations of fin control surface deflections. The angle-of-attack range was from -2 to 28 deg at constant angles of sideslip of -8, -4, 0, 4, and 8 deg. The test Reynolds number was 4.25 million, based on free-stream conditions and model length, at each		

CONFIDENTIAL

UNCLASSIFIED

20. ABSTRACT (Continued)

Mach number. Results are presented illustrating the effects of control surface deflections, Mach number, and model attitude on missile and fin aerodynamic characteristics. (U)

UNCLASSIFIED

DECLASSIFIED / UNCLASSIFIED**PREFACE**

(U) The work reported herein was conducted by the Arnold Engineering Development Center (AEDC), Air Force Systems Command (AFSC), at the request of the Air Force Armament Laboratory (AFATL/DLMA), Eglin Air Force Base, Florida, under Program Element 62602F, Project 2069, Task 01. The AFATL project monitor was Mr. Tom Noethen. The results were obtained by ARO, Inc., AEDC Division (a Sverdrup Corporation Company), operating contractor for the AEDC, AFSC, Arnold Air Force Station, Tennessee, under ARO Project Number V41A-NOA. The author of this report was D. H. Fikes, ARO, Inc. The final data package was completed on January 10, 1977, and the manuscript (ARO Control No. ARO-VKF-TR-77-17) was submitted for publication on March 21, 1977.

(U) This report contains no classified information taken from other classified documents.

DECLASSIFIED / UNCLASSIFIED

CONTENTS

	<u>Page</u>
1.0 INTRODUCTION	5
2.0 APPARATUS	
2.1 Wind Tunnel	5
2.2 Model	6
2.3 Instrumentation and Precision	6
3.0 PROCEDURE	
3.1 Test Conditions	9
3.2 Test Procedure	9
3.3 Data Reduction	10
3.4 Data Uncertainty	11
4.0 RESULTS AND DISCUSSION	14
REFERENCES	15

ILLUSTRATIONS

Figure

1. Wind Tunnel and Model Injection System	17
2. Model Photographs	18
3. Model Details	20
4. Fin Orientation and Deflection Conventions	23
5. Fin Aerodynamic Coefficient Sign Convention	24
6. Base Pressure Tap Locations	25
7. Missile Aerodynamic Coefficient Sign Convention	26
8. Pitch Control Characteristics	27
9. Yaw Control Characteristics	31
10. Roll Control Characteristics	35

TABLE

1. Test Summary	39
NOMENCLATURE	40

1.0 INTRODUCTION

(U) A static force test was conducted in the Arnold Engineering Development Center (AEDC) von Kármán Gas Dynamics Facility (VKF) Supersonic Wind Tunnel (A) on a model of a proposed maneuvering air-to-air missile (AAM). The proposed missile will incorporate advances in the state of the art of missile bank-to-turn control and missile maneuvering technology.

(U) Static stability, axial-force, and fin-loading data were obtained at Mach numbers 1.5, 2.5, and 3.5 at a test Reynolds number of 4.25 million based on model length. Fin deflections ranged from -20 to 10 deg. The angle-of-attack range was from -2 to 28 deg at constant angles of sideslip of -8, -4, 0, 4, and 8 deg.

(U) This model configuration was previously tested in Tunnel A over the same range of test conditions and is reported in Ref. 1. For this test, modifications were made to the model to include fin balances for two of the four fins. The fin force and moment data were of primary concern, and the missile aerodynamics obtained were essentially a repeat of data obtained in the previous test, reported in Ref. 1.

(U) Testing of this configuration over the transonic Mach number range was conducted in the Aerodynamic Wind Tunnel (4T) of the AEDC Propulsion Wind Tunnel Facility (PWT). Results of that testing will be covered in a separate technical report.

2.0 APPARATUS

2.1 WIND TUNNEL

(U) Tunnel A (Fig. 1) is a continuous, closed-circuit, variable density wind tunnel with an automatically driven flexible-plate-type

nozzle and a 40- by 40-in. test section. The tunnel can be operated at Mach numbers from 1.5 to 6 at maximum stagnation temperatures up to 750°R at $M_{\infty} = 6$. Minimum operating pressures range from about one-tenth to one-twentieth of the maximum at each Mach number. The tunnel is equipped with a model injection system which allows removal of the model from the test section while the tunnel remains in operation. A description of the tunnel and airflow calibration information may be found in Ref. 2.

2.2 MODEL

(U) Photographs and details of the Air Force Armament Laboratory (AFATL) Bank-to-Turn, Air-to-Air Missile Model are shown in Figs. 2 and 3. The model was designed by AFATL/DLMI and was fabricated at AEDC. Basic model components consisted of a body, wings, and fins. The model body was of elliptical cross section (Fig. 3a). The cross section was of increasing ellipticity from the nose to MS 13.125 and was of decreasing ellipticity from MS 13.125 to MS 18.900. Details of the wings are shown in Fig. 3b. The four identical tail fins (Fig. 3c) were of nearly triangular shape and were arranged in a split x shape configuration (Fig. 4) at zero model roll. Fin deflection angles were set using angle pins for ± 0 , 5, 10, 15, or 20 deg. Fin orientation and deflection conventions are shown in Fig. 4. Fins 1 and 3 were mounted to fin balances. The aerodynamic coefficient sign conventions of these fins are presented in Fig. 5.

2.3 INSTRUMENTATION AND PRECISION

(U) Tunnel A stilling chamber pressure is measured with a 15, 60, 150, or 300-psid transducer referenced to a near vacuum. Based on periodic comparisons with secondary standards, the uncertainty (a bandwidth which includes 95 percent of the residuals) of these transducers is estimated to be within ± 0.2 percent of reading or ± 0.015 psia,

whichever is greater. Stilling chamber temperature is measured with a copper-constantan thermocouple with an uncertainty of $\pm 3^\circ\text{F}$ based on repeat calibrations.

(U) Aerodynamic forces and moments on the total vehicle were measured with a six-component, moment-type strain-gage balance supplied and calibrated by VKF. Prior to the test, static loads in each plane and combined static loads were applied to the balance to simulate the range of loads and center-of-pressure locations anticipated during the test. The following uncertainties represent the bands of 95 percent of the measured residuals, based on differences between the applied loads and the corresponding values calculated from the balance calibration equations included in the final data reduction. The range of check loads applied and the measurement uncertainties follow.

Component	Balance Design Loads	Calibration Load Range	Range Of Check Loads	Measurement Uncertainty
Normal force, lb.	± 700	± 700	± 700	± 1.50
Pitching moment,* in.-lb	$\pm 3,645$	$\pm 3,645$	± 800	± 3.00
Side force, lb.	± 700	± 700	± 150	± 1.75
Yawing moment,* in.-lb.	$\pm 3,645$	$\pm 1,822$	$\pm 1,120$	± 5.00
Rolling moment, in.-lb.	± 320	± 200	± 300	± 0.80
Axial force, lb.	150	150	25 to 100	± 1.10

*About balance forward-moment bridge.

(U) The transfer distance from the balance forward-moment bridge to the model moment reference location was 2.020 in. along the longitudinal axis and was measured with an estimated precision of ± 0.005 in.

(U) Aerodynamic loads on the two instrumented fins were measured with five-component force- and moment-type balances supplied by AFATL

UNCLASSIFIED

AEDC-TR-77-43

and calibrated by VKF. Prior to the test, static loads in each plane and combined static loads were applied to each balance to simulate the range of loads and center-of-pressure locations anticipated during the test. The uncertainties listed below were determined in the same manner as were the balance uncertainties for the total vehicle. The fin balance number indicates the balance location (see Fig. 5).

Component	Design Loads	Calibration Loads	Check Loads	Measurement Uncertainty	
	Fin Balances 1 and 3	Fin Balances 1 and 3	Fin Balances 1 and 3	Fin Balances 1 and 3	Fin Balances 1 and 3
Normal Force, lb.	± 60	± 40	±20	±0.54	±0.63
Hinge Moment, in.-lb*	±166	±115	±10	±0.80	±0.30
Bending Moment, in.-lb	±130	±100	±10	±0.55	±0.53

*About balance forward-moment bridge.

The transfer distance from the fin balance forward-moment bridge to the fin hinge line was 1.864 and 1.888 in. for fins 1 and 3, respectively. The transfer distance from the fin balance reference location to the theoretical fin root chord (body surface) was 0.571 and 0.576 in. for fins 1 and 3, respectively. Each transfer distance was measured with an estimated precision of ±0.005 in.

(U) Base pressures were measured with 15-psid transducers referenced to a near vacuum and having full-scale calibrated ranges of 1, 5, and 15 psia. Based on periodic comparisons with secondary standards, the uncertainty is estimated to be ±0.1 percent of full scale of the range being used. Base pressure tap locations are shown in Fig. 6.

(U) Shadowgraphs were obtained on all configurations at selected model attitudes. The shadowgraphs were recorded with a double pass optical flow visualization system with a 35-in.-diam field of view.

3.0 PROCEDURE

3.1 TEST CONDITIONS

(U) The test was conducted at free-stream Mach numbers 1.51, 2.50, and 3.51. The free-stream Reynolds number, based on a model length of 18.900 in., was 4.25 million. A summary of the test conditions at each Mach number is given below.

M_∞	P_o , psia	T_o , °R	q_∞ , psia	p_∞ , psia	$Re_{\ell_m} \times 10^{-6}$
1.51	9.5	570	4.1	2.64	4.25
2.50	14.5	↓	3.7	0.85	↓
3.51	24.2	↓	2.8	0.32	↓

(U) A test summary showing all configurations tested and the variables for each is presented in Table 1.

3.2 TEST PROCEDURE

(U) In Tunnel A, the model is mounted on a sting support mechanism located in an installation tank directly underneath the tunnel test area. The installation tank is separated from the tunnel by a pair of fairing doors and a safety door. When closed, the fairing doors cover the opening to the tank (except for a slot for the pitch sector), and the safety door seals the tunnel from the tank area. After the model is prepared for a data run, the personnel access door to the installation tank is closed, the tank is vented to the tunnel flow, and the safety and fairing doors are opened. Then the model is injected into the airstream, and after it reaches tunnel centerline, it is translated forward into the test section. After the data run is completed, the model is returned into the tank, and the fairing and safety doors are closed, sealing the tank from the tunnel. The tank is then vented to

atmosphere with the tunnel running to allow access to the model in preparation for the next run. The sequence is repeated after each configuration or test condition change.

(U) Model attitude positioning and data recording were accomplished with the pitch-pause mode of operation. The VKF Model Attitude Control System (MACS) was used and greatly increased the data acquisition rate. Model pitch and roll requirements were entered into the controlling computer before the test was begun. Model positioning and data recording operations were performed automatically during the test by selecting the list of desired model attitudes and initiating the system. At each model attitude, the control system delayed the data acquisition sequence until the base pressures had time to stabilize.

(U) Data were sampled at a rate of 1,500 channels/sec, and 20 data loops were averaged for each data point. Data were obtained for the angle-of-attack range from -2 to 28 deg at sideslip angles of -8, -4, 0, 4, and 8 deg.

3.3 DATA REDUCTION

(U) Missile and fin static force data (16 channels) were obtained simultaneously, utilizing the high-speed scanning capability of the data acquisition system available in Tunnel A. Missile and fin force and moment measurements were reduced to coefficient form using the values calculated from the averaged data points and corrected for first- and second-order balance interaction effects. Missile coefficients also were corrected for model tare weight and balance-sting deflections. Only fin tare weight corrections were applied to the fin coefficients, since the fin deflection effects were negligible. Model attitude, base pressure, and tunnel pressure and temperature were also calculated from averaged values.

(U) Missile aerodynamic force and moment coefficients are presented in the body axis system. Pitching- and yawing-moment coefficients are referenced to a point on the model centerline 10.998 in. from the model nose (see Fig. 3a). The coefficient reference area was the maximum body cross-sectional area. The coefficient reference length was defined to be the diameter of a circle with an area equal to the reference area. Forebody axial-force coefficients (C_A) have been adjusted to zero base axial force using measured model base pressures obtained and applied as described in section 3.2.

(U) Fin aerodynamic force and moment coefficients are presented in the fin axis system. The fin normal force is normal to the plane defined by the fin hinge line and root chord centerline. Fin spanwise bending moment is referenced to the theoretical root chord (model surface) at each fin location. Fin hinge moment is referenced to the fin hinge line (see Fig. 3c). Reference lengths and areas for the fin aerodynamic coefficients were the same as those used for the missile aerodynamic coefficients. The sign convention for the fin aerodynamic coefficients is shown in Fig. 5.

3.4 DATA UNCERTAINTY

(U) An evaluation of the influence of random measurement errors is presented in this section to provide a partial measure of the uncertainty of the final test results presented in this report. Although evaluation of the systematic measurement error (bias) is not included, it should be noted that the instrumentation precision values (given in Section 2.3) used in this evaluation represent a total uncertainty combination of both systematic and two-sigma random error contributions.

3.4.1 Test Conditions

(U) Uncertainties in the basic tunnel parameters P_0 and T_0 (see

Section 2.3) and the two-sigma deviation in Mach number determined from test section flow calibrations were used to estimate uncertainties in the other free-stream properties, using the Taylor series method of error propagation.

Uncertainty (\pm), percent						
M_∞	M_∞	P_o	T_o	P_∞	q_∞	$Re_{\ell_m} \times 10^{-6}$
1.51	1.3	0.2	0.5	2.9	0.3	0.8
2.50	0.8	0.2	0.5	3.0	1.5	1.3
3.51	0.5	0.2	0.5	2.8	1.7	1.3

3.4.2 Aerodynamic Coefficients

(U) The uncertainty of the aerodynamic coefficients was estimated by using the Taylor series method of error propagation to combine the balance and base pressure uncertainties listed in Section 2.3 with uncertainties in the tunnel parameters. The aerodynamic coefficient uncertainties thus obtained are presented below.

Uncertainty (\pm)							
Maximum Measured Coefficient Value, percent							
M_∞	C_N	C_m	C_Y	C_n	C_ℓ	C_A	C_{A_t}
1.51	0.5	1.0	1.8	1.2	1.1	2.3	1.9
2.50	1.6	2.4	3.1	2.5	1.9	3.9	3.2
3.51	1.9	3.2	4.2	3.4	2.1	4.7	4.3

(U) The basic precision of the aerodynamic coefficients was also computed using only the balance and base pressure uncertainties listed in Section 2.3 along with the nominal test conditions; it was assumed

~~CONFIDENTIAL~~

REF ID: A70000

that the free-stream flow nonuniformity is a bias type of uncertainty which is constant for all test runs. These values therefore represent the data repeatability expected and are especially useful for detailed discrimination purposes in parametric model studies.

M_∞	Repeatability (\pm)						
	Measured Coefficient Value						
M_∞	C_N	C_m	C_Y	C_n	C_l	C_A	C_{A_t}
1.51	0.028	0.018	0.032	0.027	0.008	0.024	0.020
2.50	0.030	0.019	0.035	0.029	0.008	0.026	0.022
3.51	0.039	0.025	0.046	0.038	0.008	0.029	0.029

(U) The fin aerodynamic coefficient uncertainties were determined in the same manner as were the total body aerodynamic coefficient uncertainties. Uncertainty values for each fin are presented below.

M_∞	Uncertainty (\pm)					
	Maximum Measured Coefficient Value, percent*					
	Fin Balance Number 1			Fin Balance Number 3		
M_∞	C_{N_F}	C_{h_F}	C_{b_F}	C_{N_F}	C_{h_F}	C_{b_F}
1.51	2.39	---	1.65	2.00	---	1.16
2.50	4.42	---	3.11	2.75	---	1.99
3.51	8.15	---	5.18	3.52	---	2.28

*Uncertainties for the C_{h_F} fin coefficients are not presented, as the maximum moments measured for these components were generally of the order of magnitude of the fin balance repeatabilities presented in the following tabulation.

DECLASSIFIED / UNCLASSIFIED

DECLASSIFIED / UNCLASSIFIED

Repeatability (\pm)
Minimum Measured Coefficient Value

M_∞	Fin Balance Number 1			Fin Balance Number 3		
	C_{N_F}	C_{h_F}	C_{b_F}	C_{N_F}	C_{h_F}	C_{b_F}
1.51	0.0093	0.0074	0.0035	0.0109	0.0061	0.0036
2.50	0.0104	0.0094	0.0039	0.0121	0.0068	0.0040
3.51	0.0137	0.0108	0.0052	0.0160	0.0089	0.0053

(U) The uncertainty in model attitude as determined from tunnel sector calibrations and consideration of the possible errors in model deflection calculations is estimated to be ± 0.1 deg in model angle of attack (α) and ± 0.1 deg in sideslip angle (β).

4.0 RESULTS AND DISCUSSION

(U) The objective of this wind tunnel test program was to determine missile and fin static aerodynamic characteristics for a proposed maneuvering air-to-air missile at supersonic Mach numbers. Experimental static force and moment data were obtained on the missile and on two of the four tail fins at Mach numbers 1.5, 2.5, and 3.5, and at a free-stream Reynolds number (Re_{ℓ_m}) of 4.25 million. Variations in model attitude and control surface deflection were investigated.

(U) Other than the fin-loading measurements, the missile aerodynamic data of this test were a repeat of data from an earlier test documented in Ref. 1. Agreement between the two sets of data is good and is within the data uncertainty given in Section 3.4.2. To keep this report complete, however, the missile stability and axial-force data are presented along with the corresponding fin-loading characteristics for fin pitch, yaw, and roll control deflections. These results are given for Mach numbers 1.5 and 3.5 in Figs. 8 through 10.

DECLASSIFIED / UNCLASSIFIED

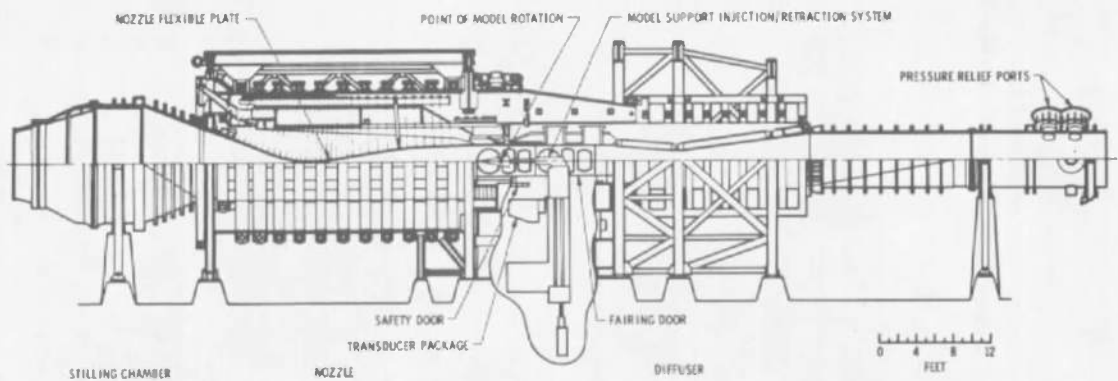
(c) Results for various control surface deflections are shown in Fig. 8. Fin normal-force, root-bending-moment, and hinge-moment coefficients are shown in Figs. 8c and d for fins numbered 1 and 3, respectively. The loading on the upper fin, fin number 1, decreases rather abruptly when the fin moves into the shadow of the wing and body, especially at $M_\infty = 1.5$.

(d) The fin-loading trends of the lower (windward) side fin, number 3 (Fig. 8d), were uniform for the various fin deflections over the angle-of-attack range at both Mach numbers. At $M_\infty = 3.5$ it is noteworthy that the angle-of-attack effect decreases with negative fin deflections so that for $\delta_p = -15$ deg the fin loading is essentially constant over the angle-of-attack range.

(e) Results for yaw control deflections given in Fig. 9 show a reduction in fin effectiveness above $\alpha = 15$ deg at Mach number 1.5; this reduction is further amplified by sideslip angle. However, the forces and moments associated with these yaw control deflections were greater than those produced by the pitch control deflections of Fig. 8. Roll control deflection data in Fig. 10 again show the decrease in fin effectiveness above $\alpha = 15$ deg (fin number 1) at Mach number 1.5. Note that the positive δ_A commands for fin number 3 correspond to the negative yaw command deflections (see Fig. 4) and that the fin loadings are identical when compared with Fig. 9d.

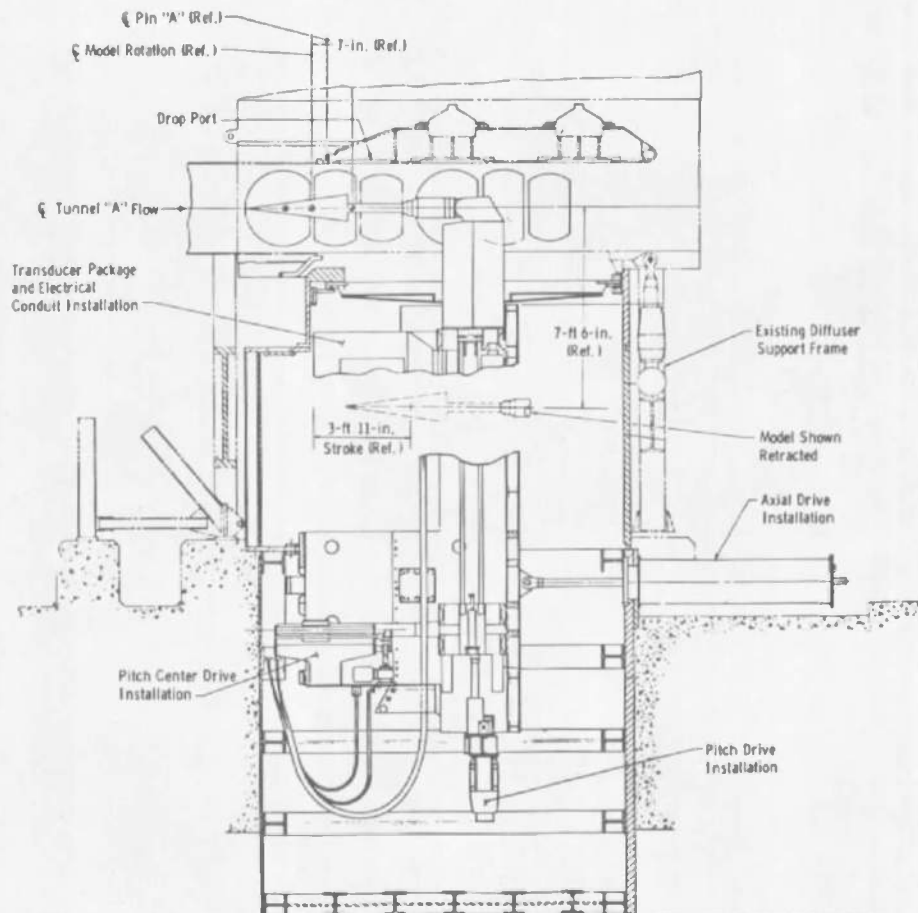
REFERENCES

1. Wannenwetsch, G. D. "Supersonic Aerodynamic Characteristics of an Advanced Concept in Air-to-Air Missile Design (U)." AEDC-TR-76-52 (ADC005740L), April 1976 (CONFIDENTIAL).
2. Test Facilities Handbook (Tenth Edition). "von Kármán Gas Dynamics Facility, Vol. 3." Arnold Engineering Development Center, May 1974.



UNCLASSIFIED

a. VKF Tunnel A



UNCLASSIFIED

b. Model injection system

Figure 1. Wind tunnel and model injection system.

UNCLASSIFIED

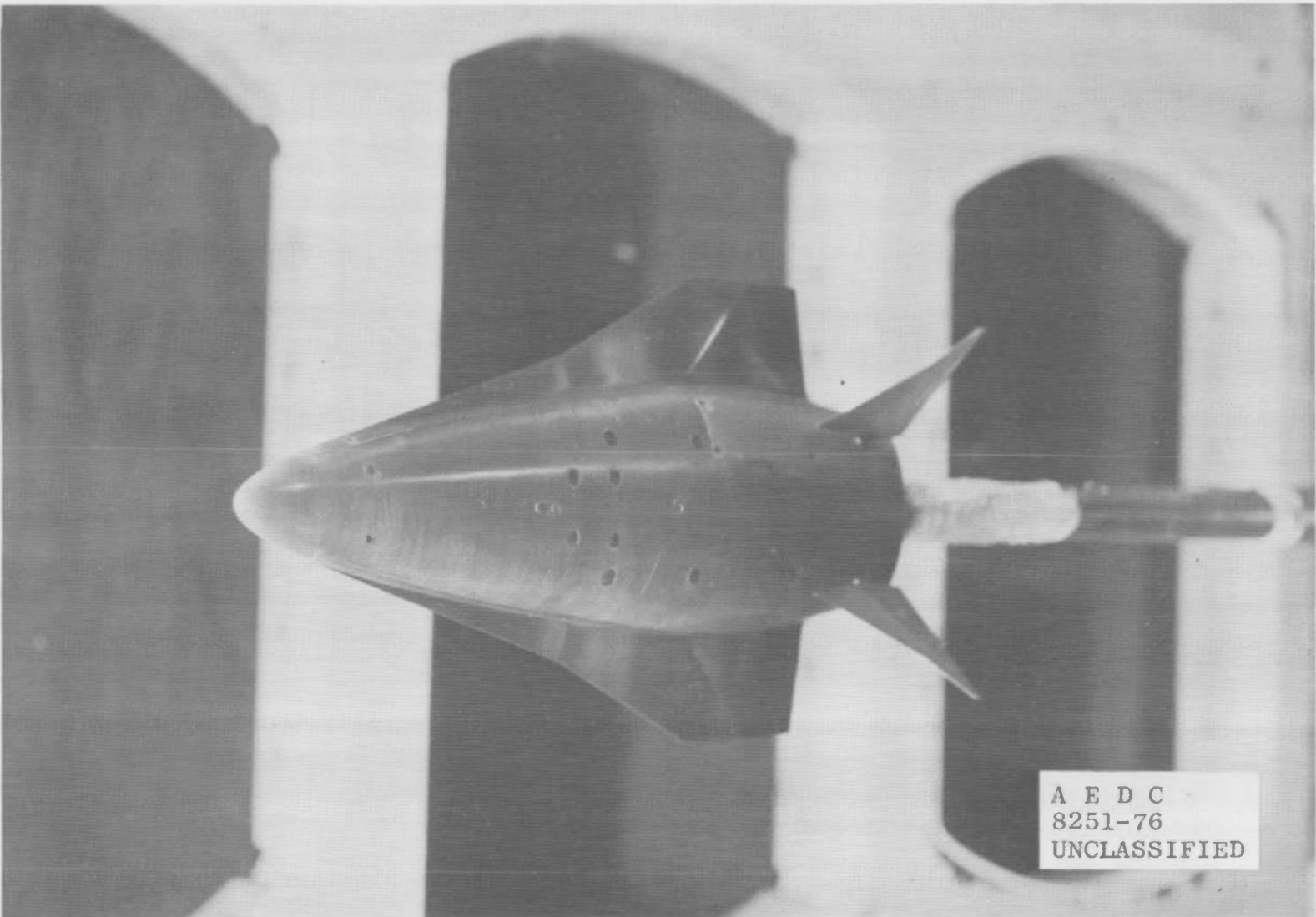


Figure 2. Model photographs.

UNCLASSIFIED

UNCLASSIFIED

AEDC-TR-77-43

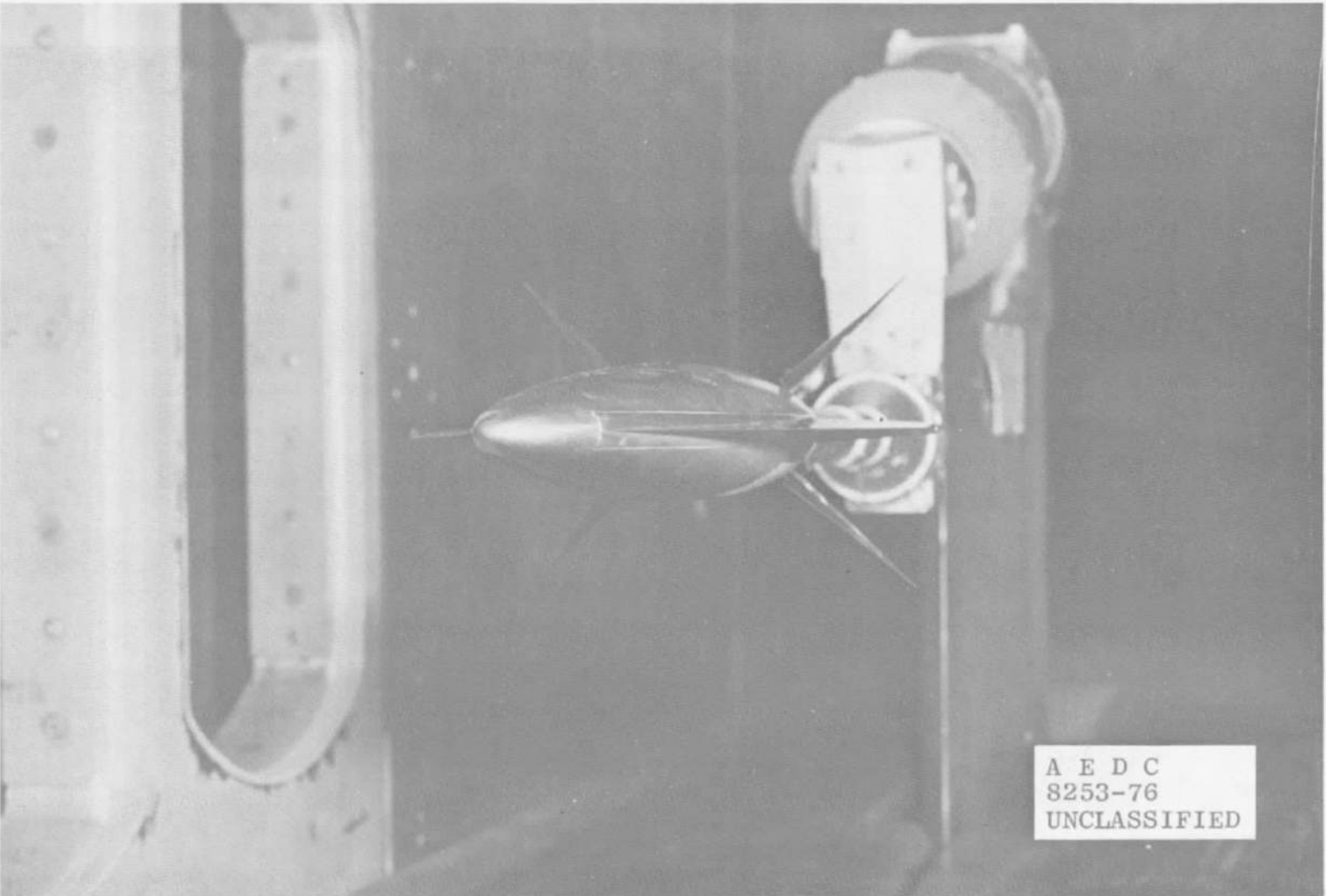
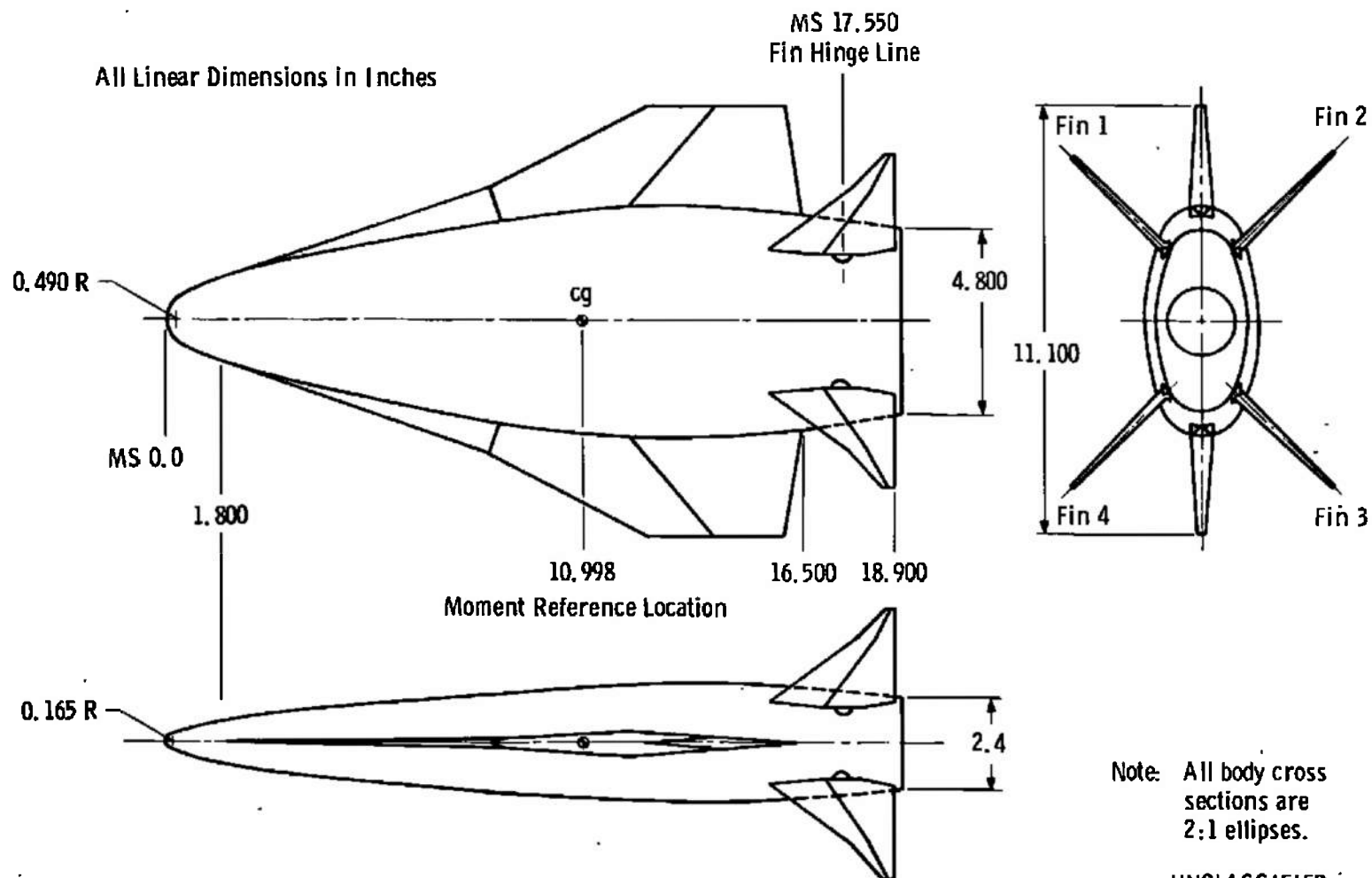


Figure 2. Concluded.

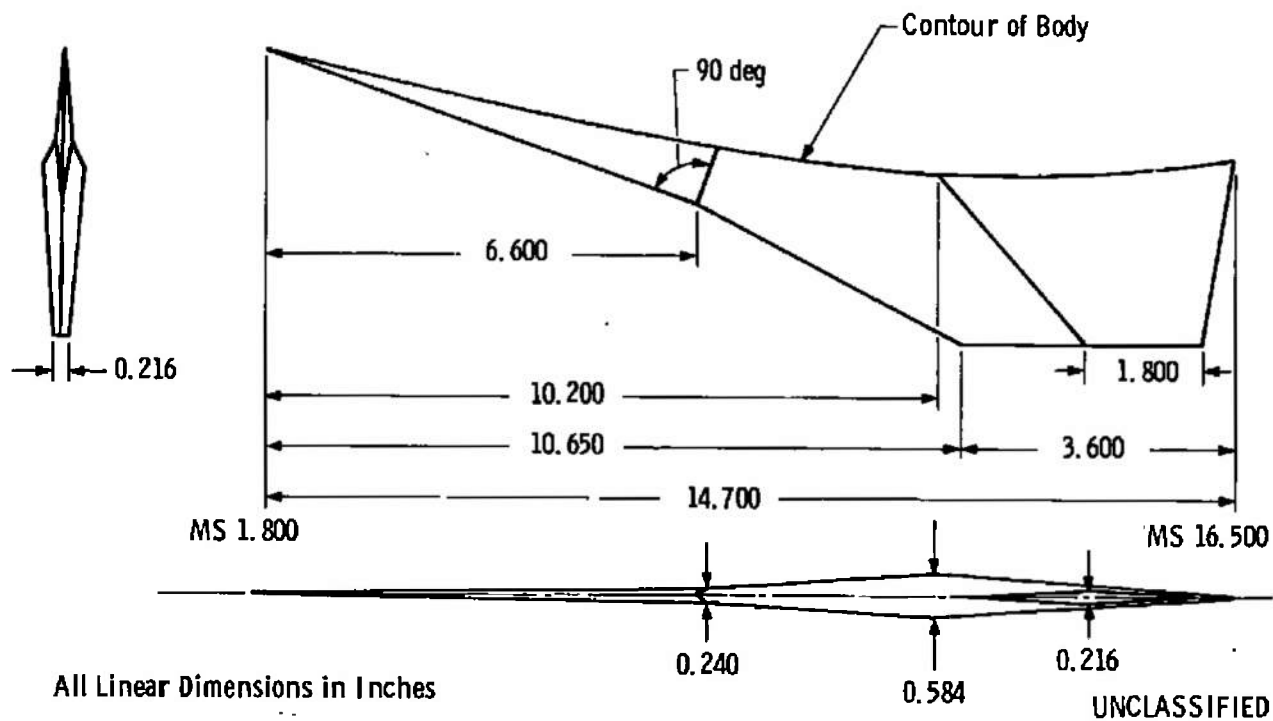
UNCLASSIFIED



UNCLASSIFIED

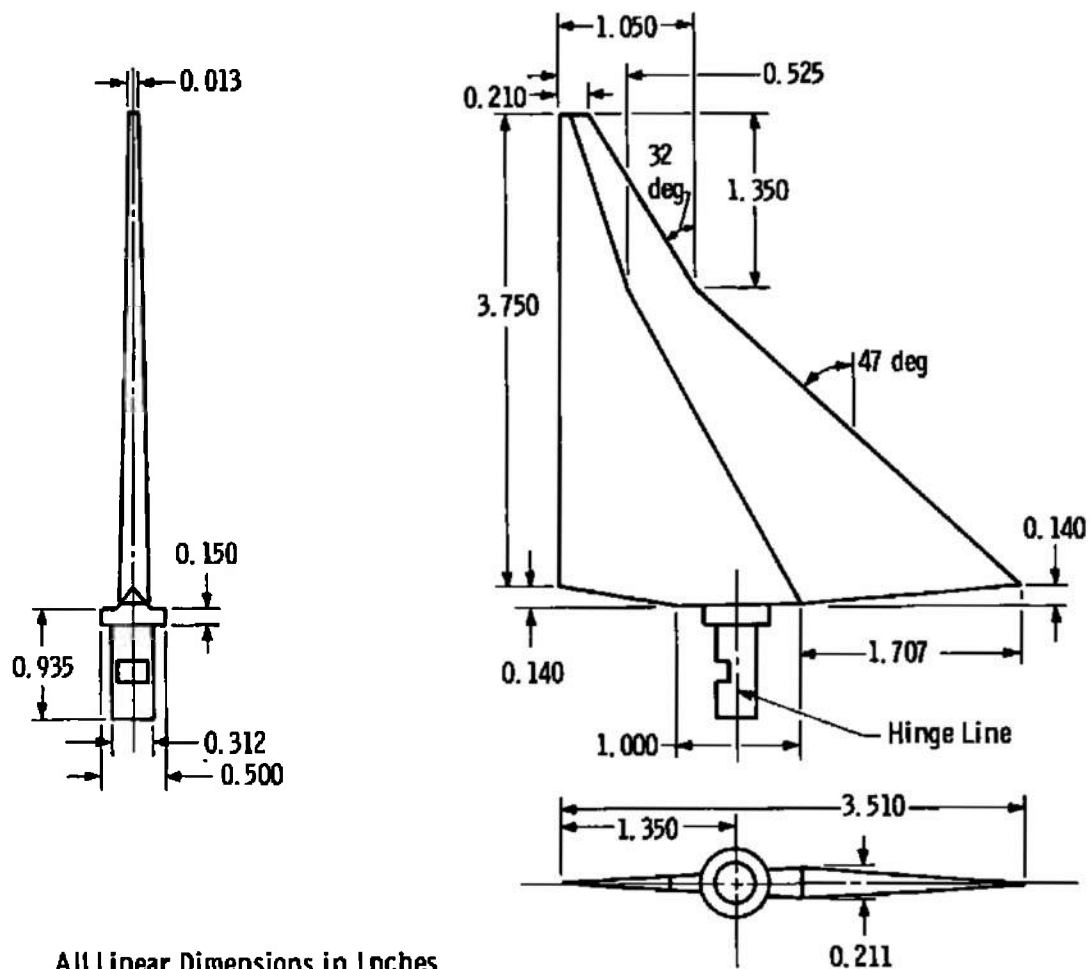
a. Configuration BWF
Figure 3. Model details.

UNCLASSIFIED



b. Wing detail
Figure 3. Continued.

UNCLASSIFIED

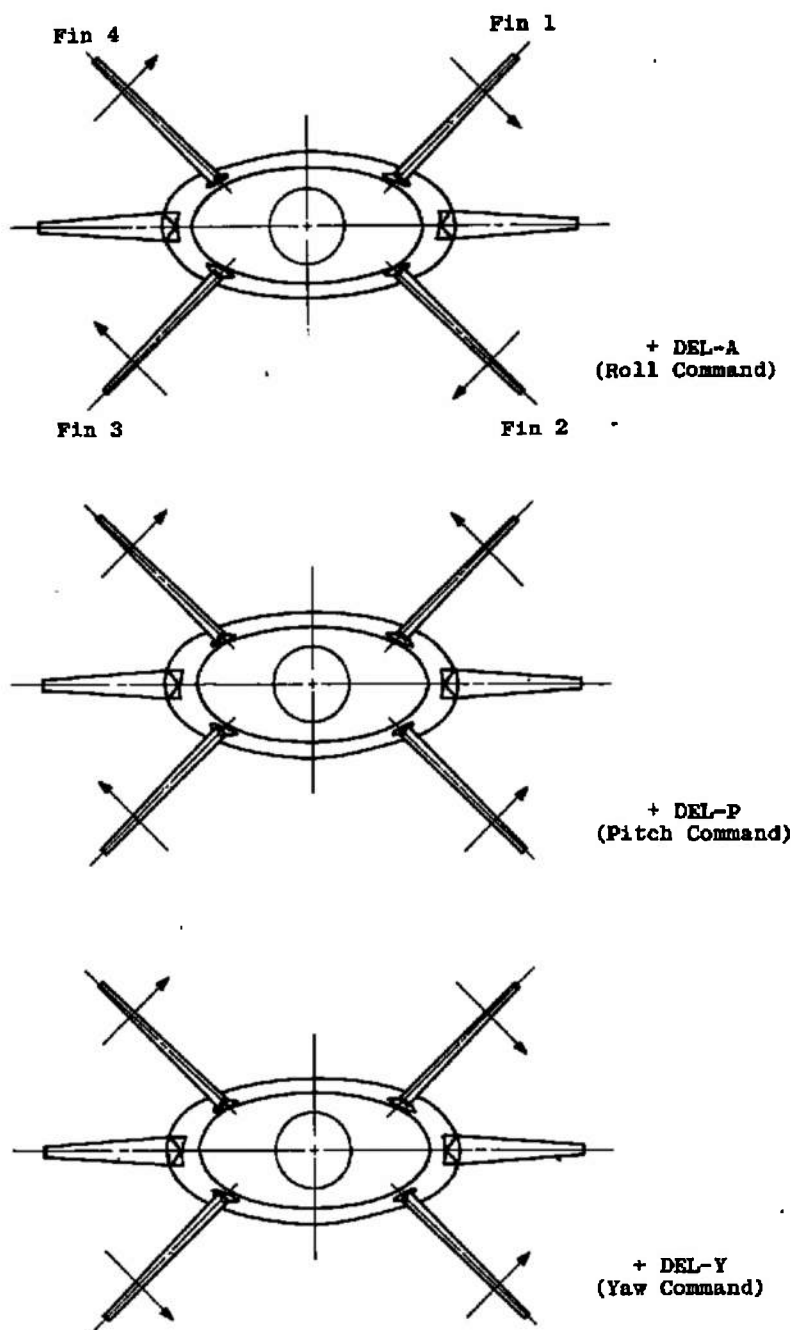


All Linear Dimensions in Inches

UNCLASSIFIED

c. Fin detail
Figure 3. Concluded.

UNCLASSIFIED

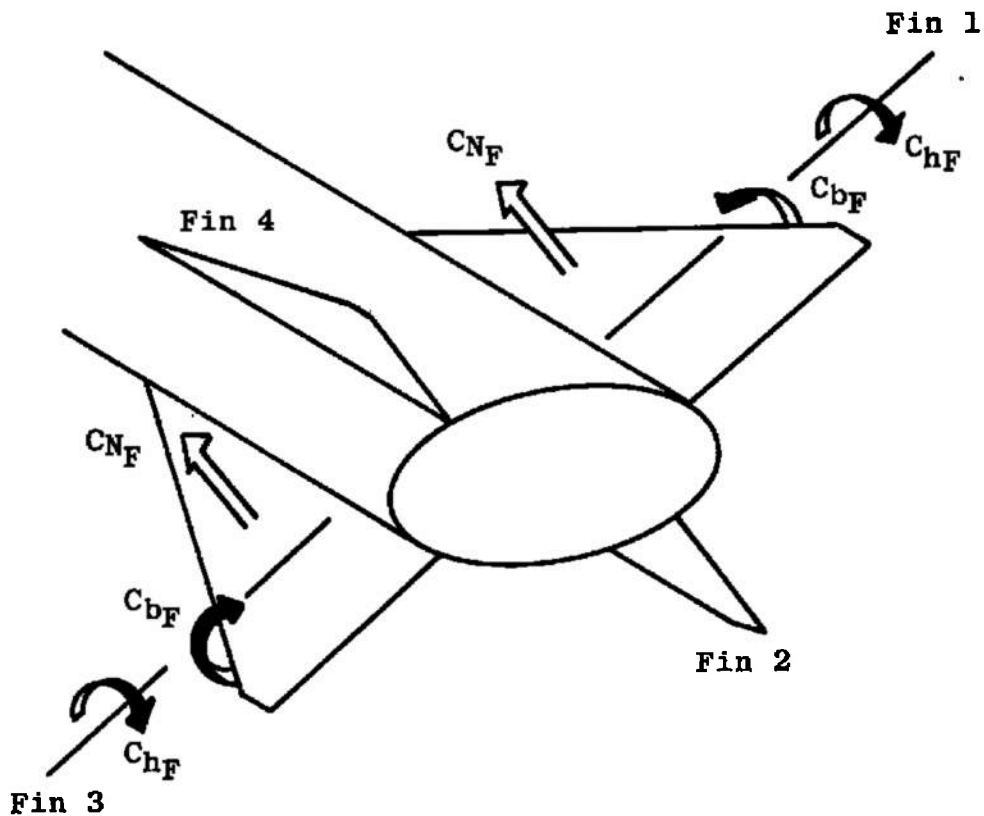


View Looking Upstream

Arrows Indicate Direction of Deflection of Leading Edge

UNCLASSIFIED

Figure 4. Fin orientation and deflection conventions.

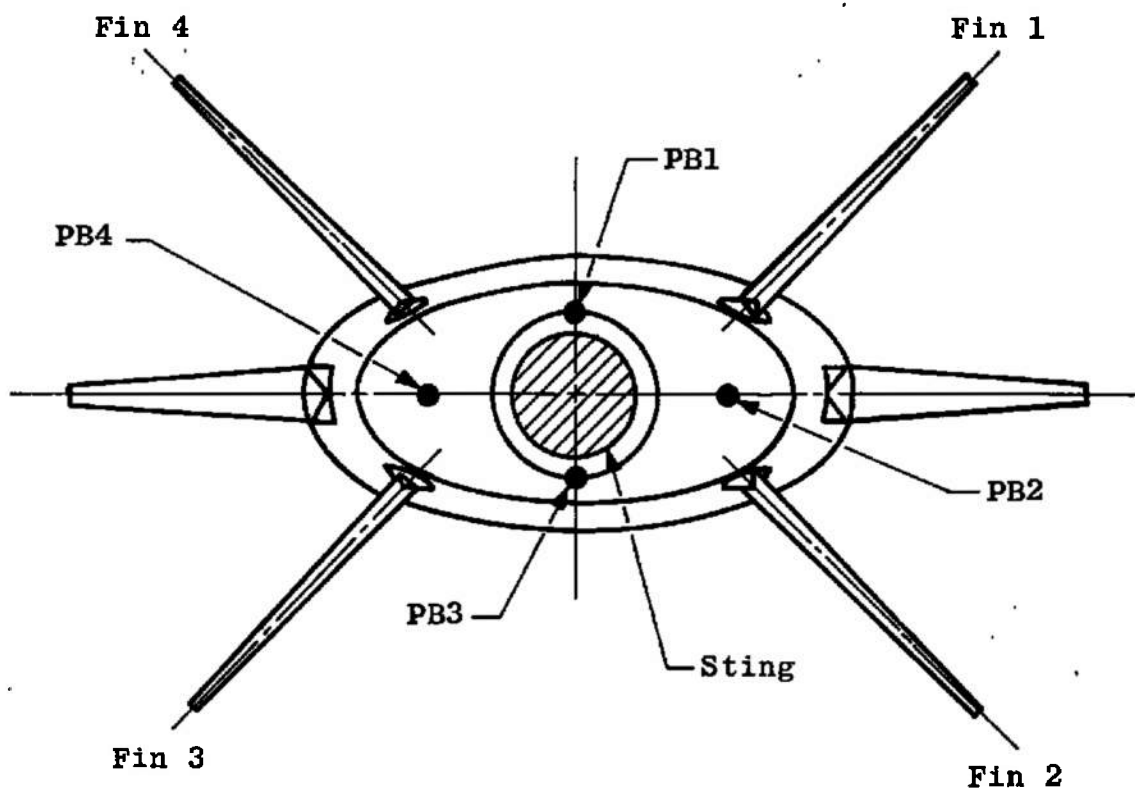


NOTE: Positive fin deflection is in same sense as positive Ch_F .

Only fins 1 and 3 were instrumented.

UNCLASSIFIED

Figure 5. Fin aerodynamic coefficient sign convention.



View Looking Upstream

UNCLASSIFIED

Figure 6. Base pressure tap locations.

UNCLASSIFIED

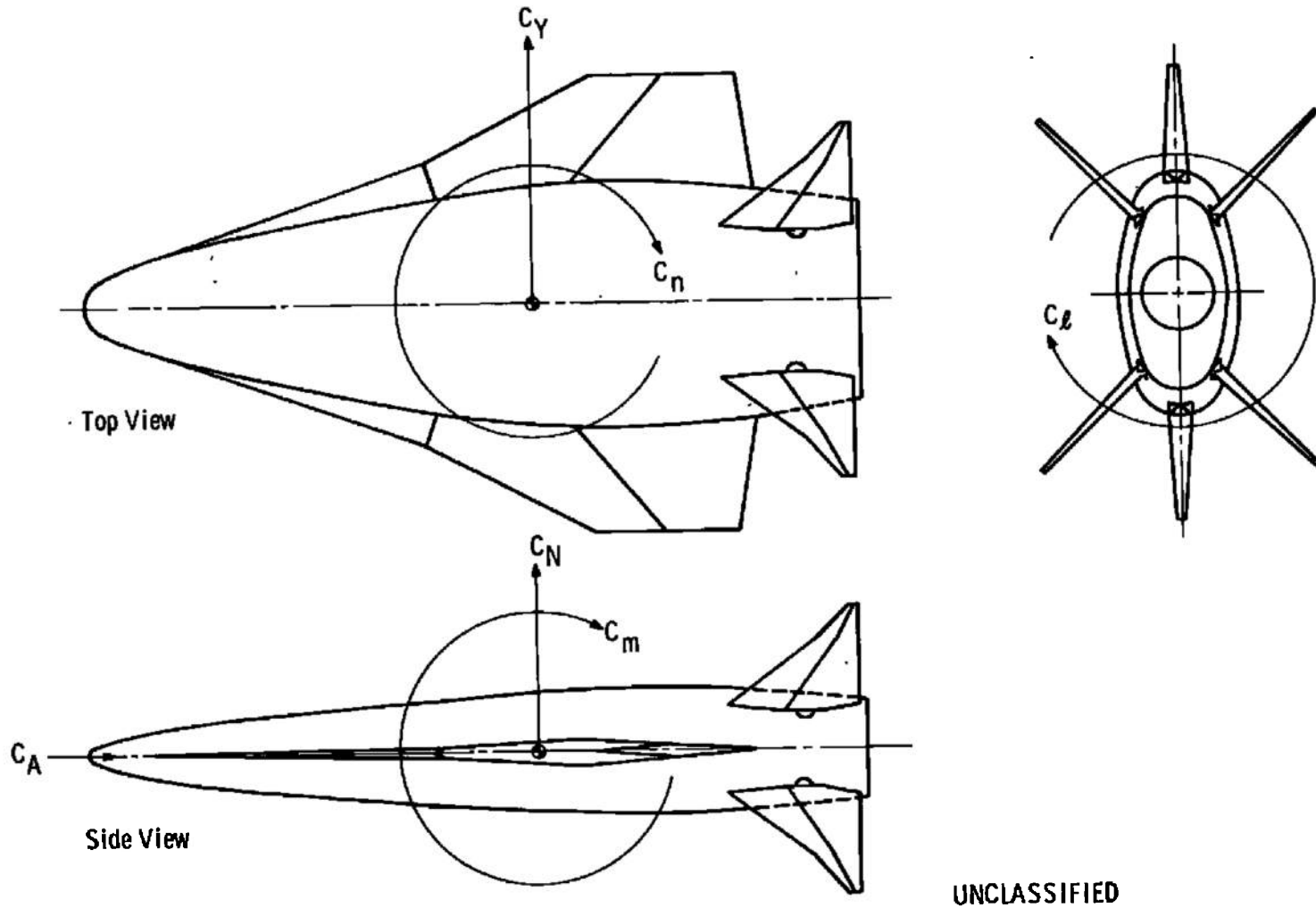
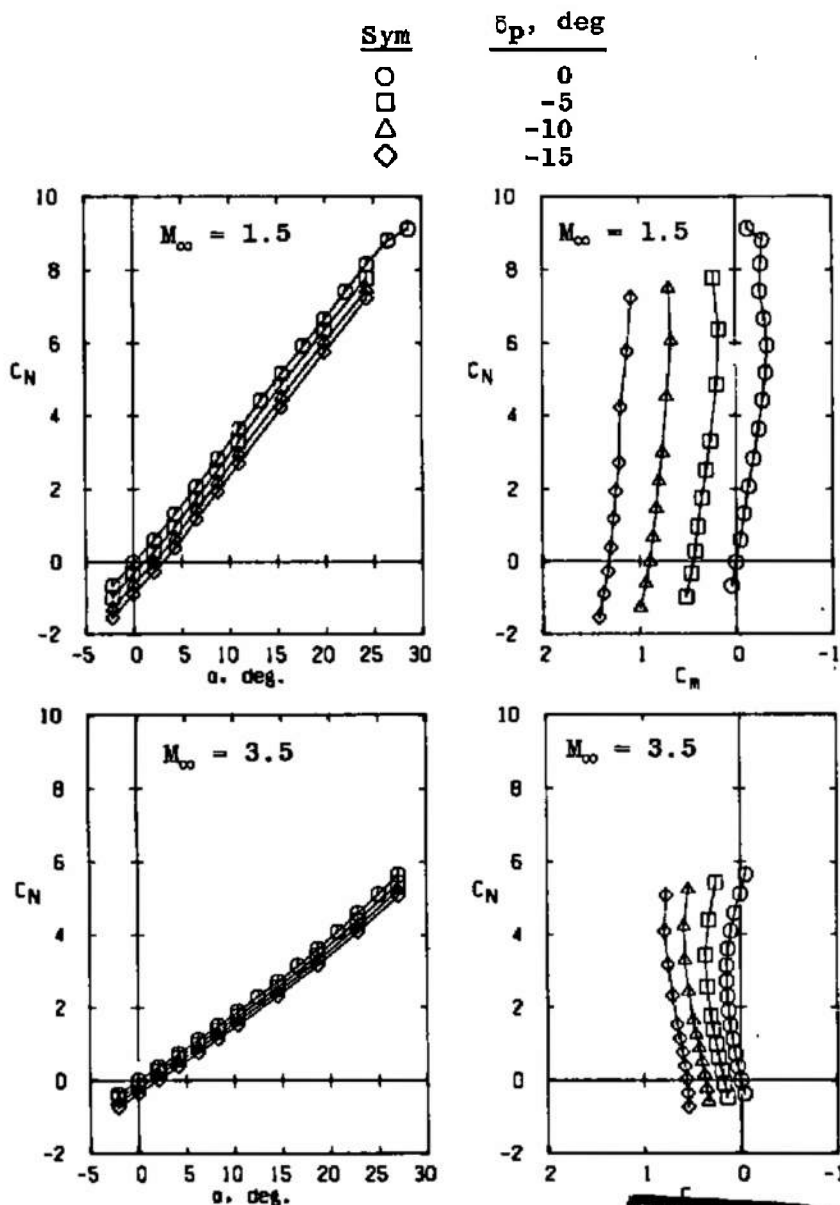


Figure 7. Missile aerodynamic coefficient sign convention.

UNCLASSIFIED

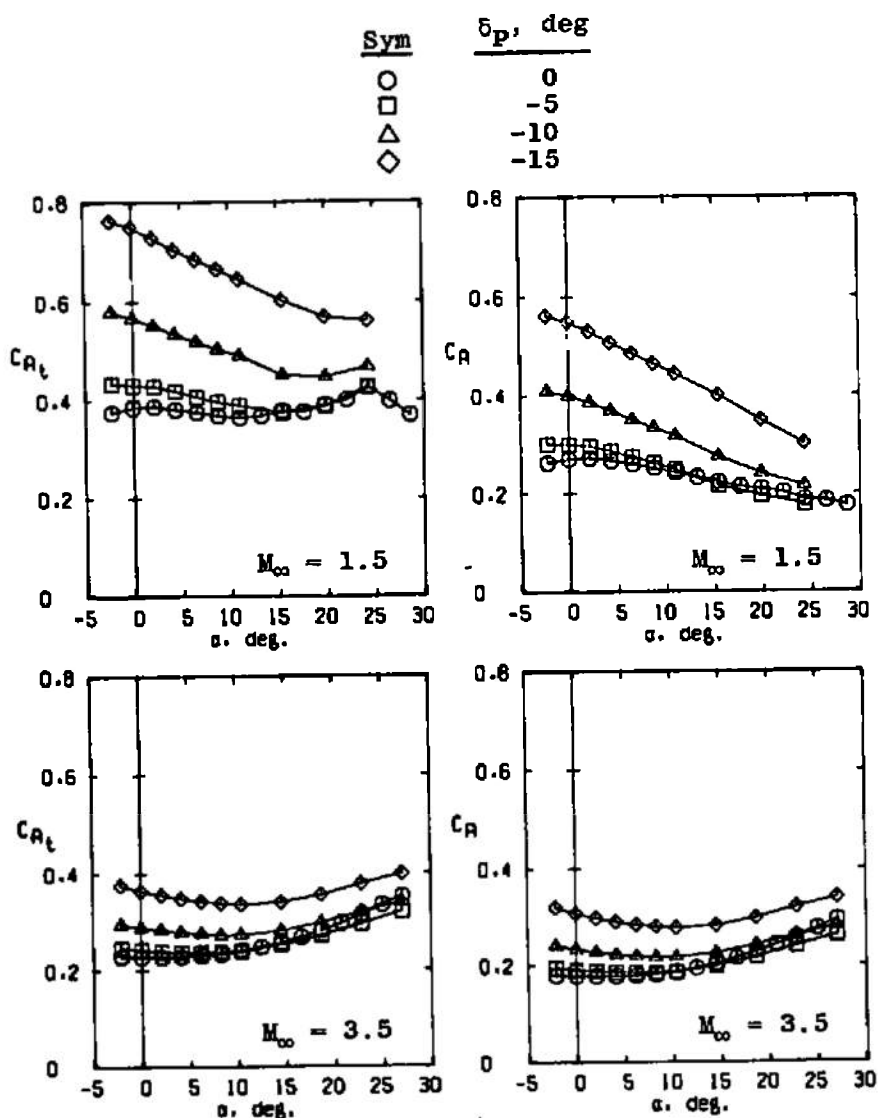
CONFIDENTIAL



a. Missile longitudinal stability
Figure 8. Pitch control characteristics.

~~CONFIDENTIAL~~

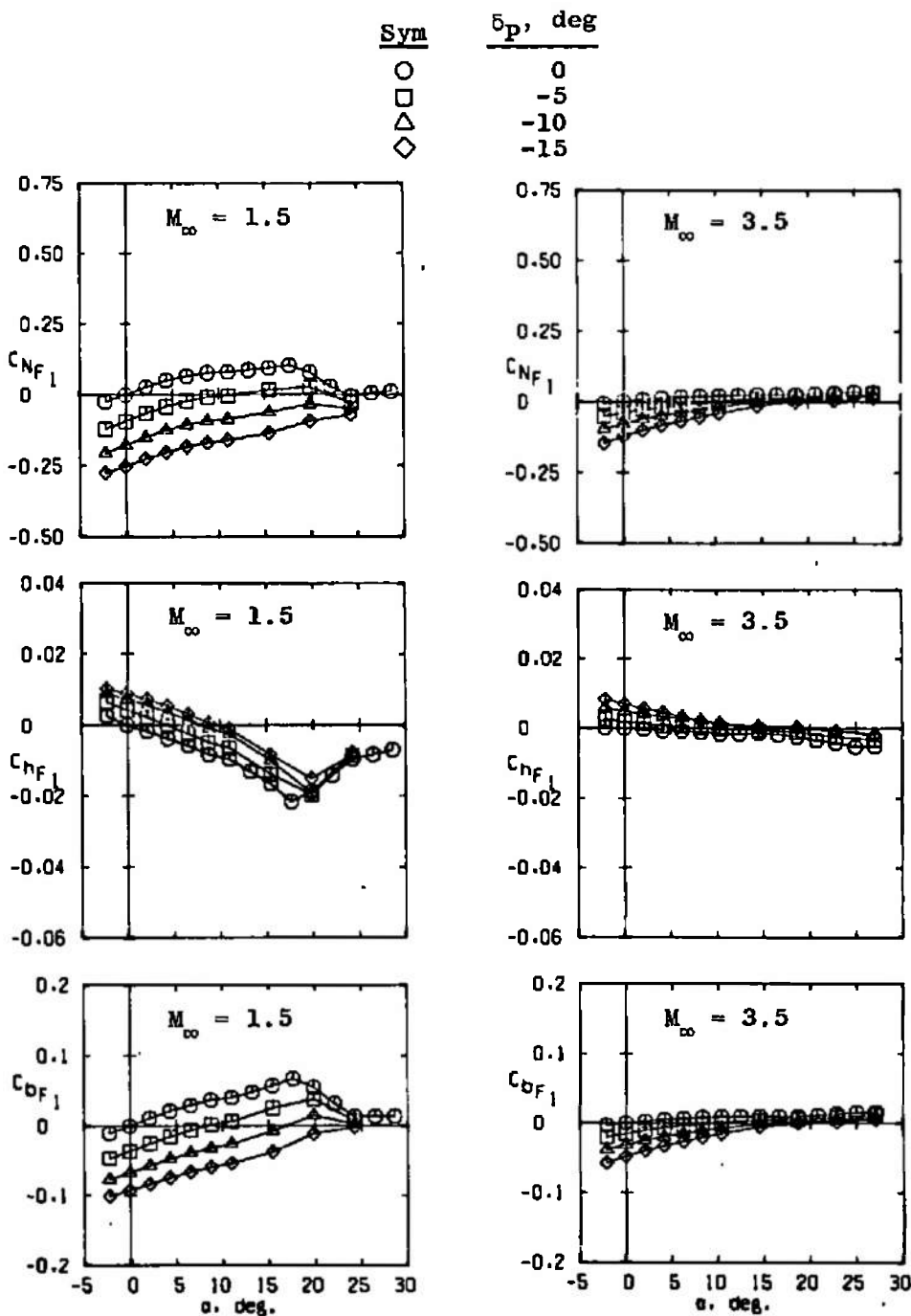
DECLASSIFIED / UNCLASSIFIED



b. Missile axial force
Figure 8. Continued.

DECLASSIFIED / UNCLASSIFIED

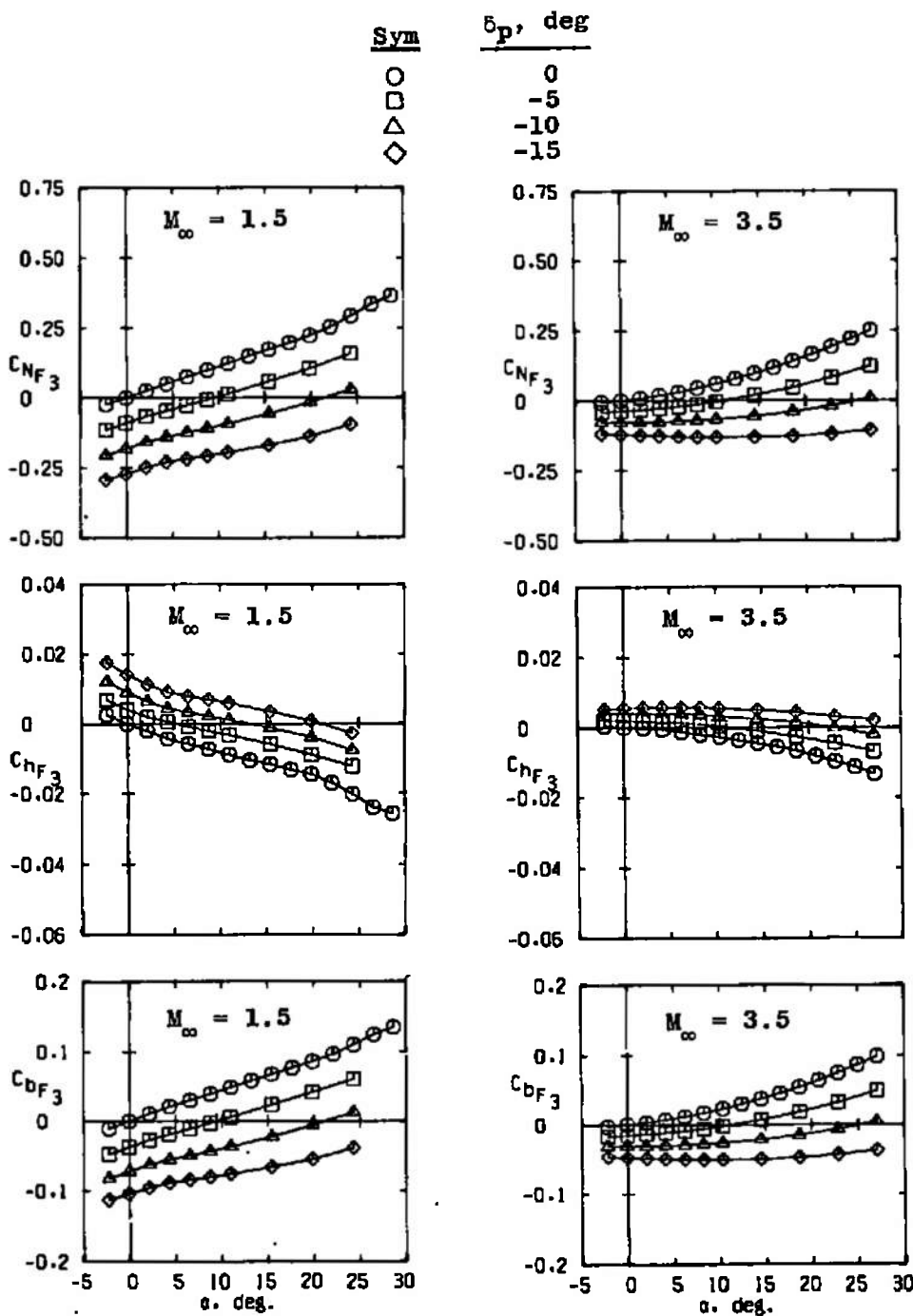
~~CONFIDENTIAL~~



c. Fin 1 aerodynamic coefficients
Figure 8. Continued.

~~CONFIDENTIAL~~

DECLASSIFIED / UNCLASSIFIED

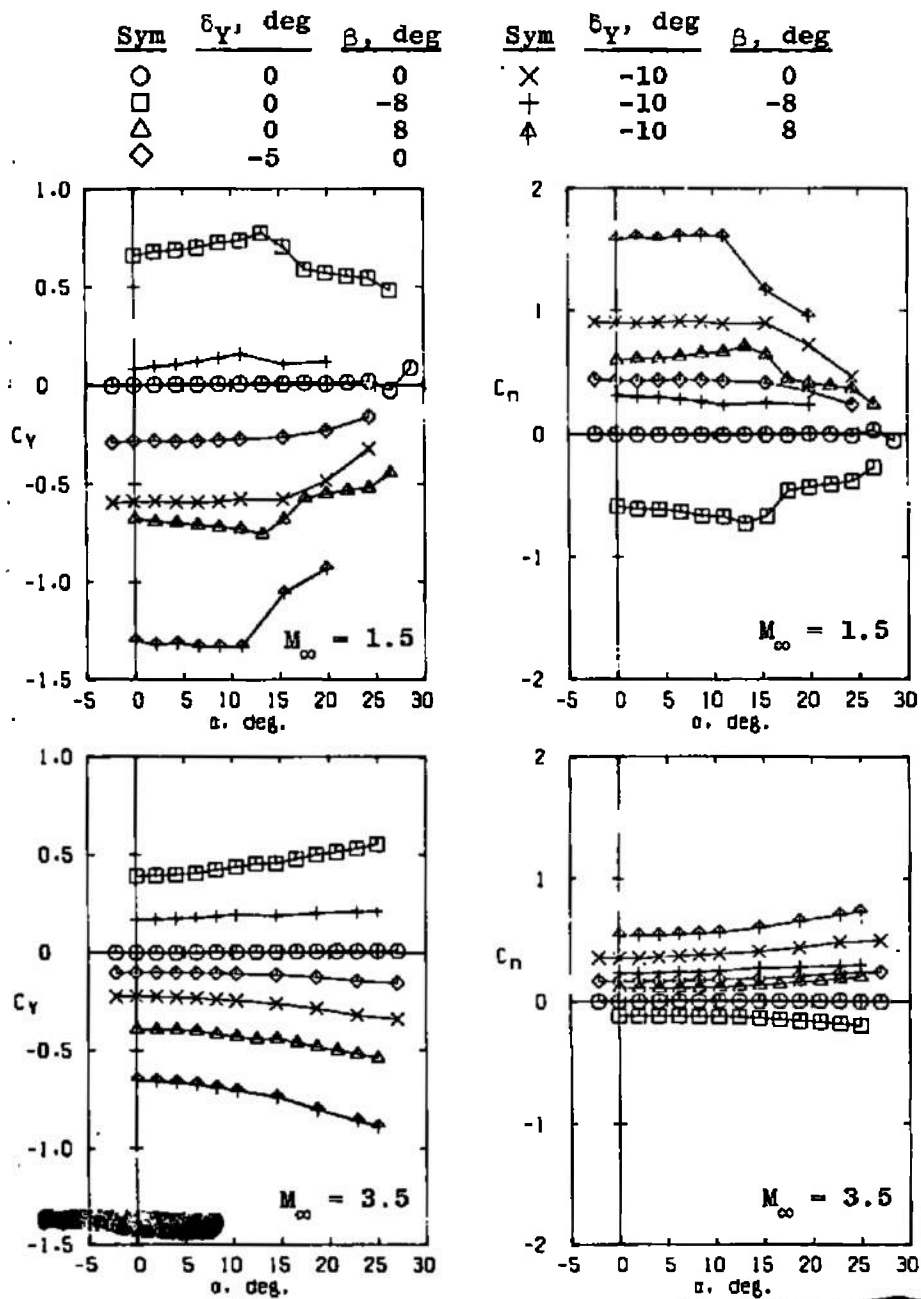


d. Fin 3 aerodynamic coefficients
Figure 8. Concluded.

DECLASSIFIED / UNCLASSIFIED

~~CONFIDENTIAL~~

DECLASSIFIED / UNCLASSIFIED

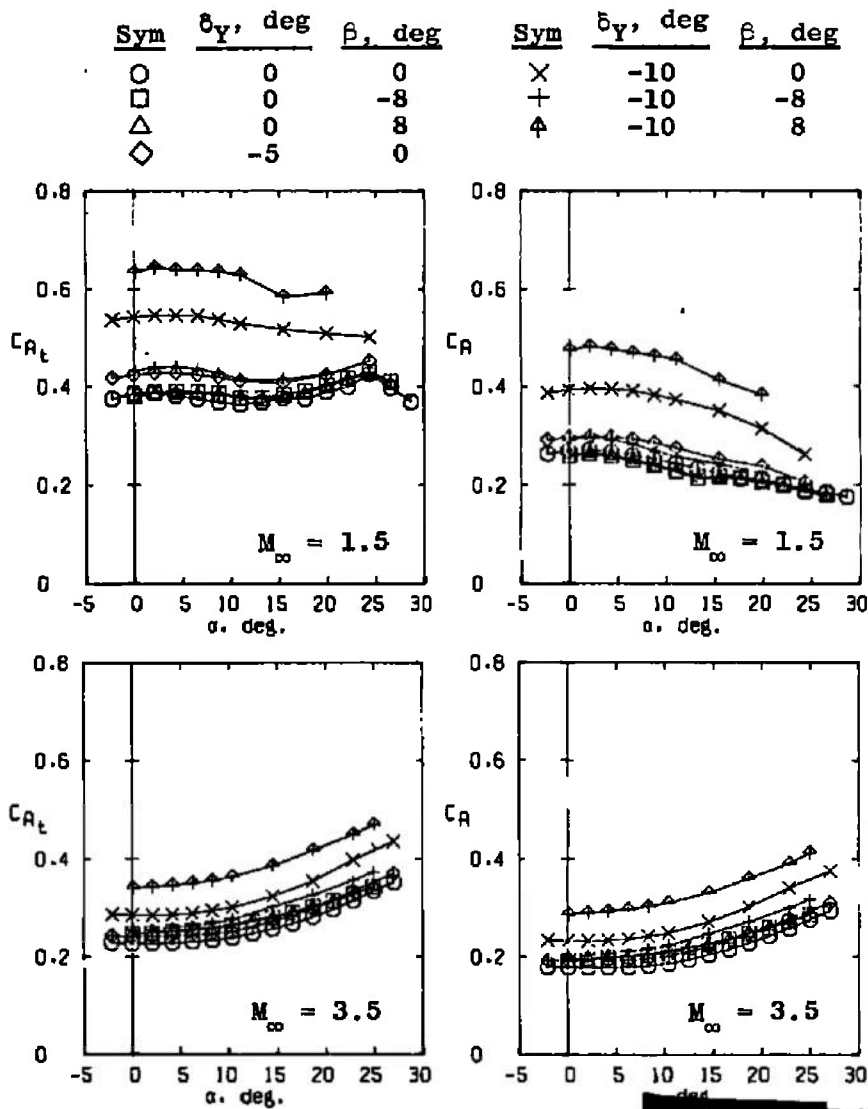


a. Missile lateral stability
Figure 9. Yaw control characteristics.

DECLASSIFIED / UNCLASSIFIED

CONFIDENTIAL

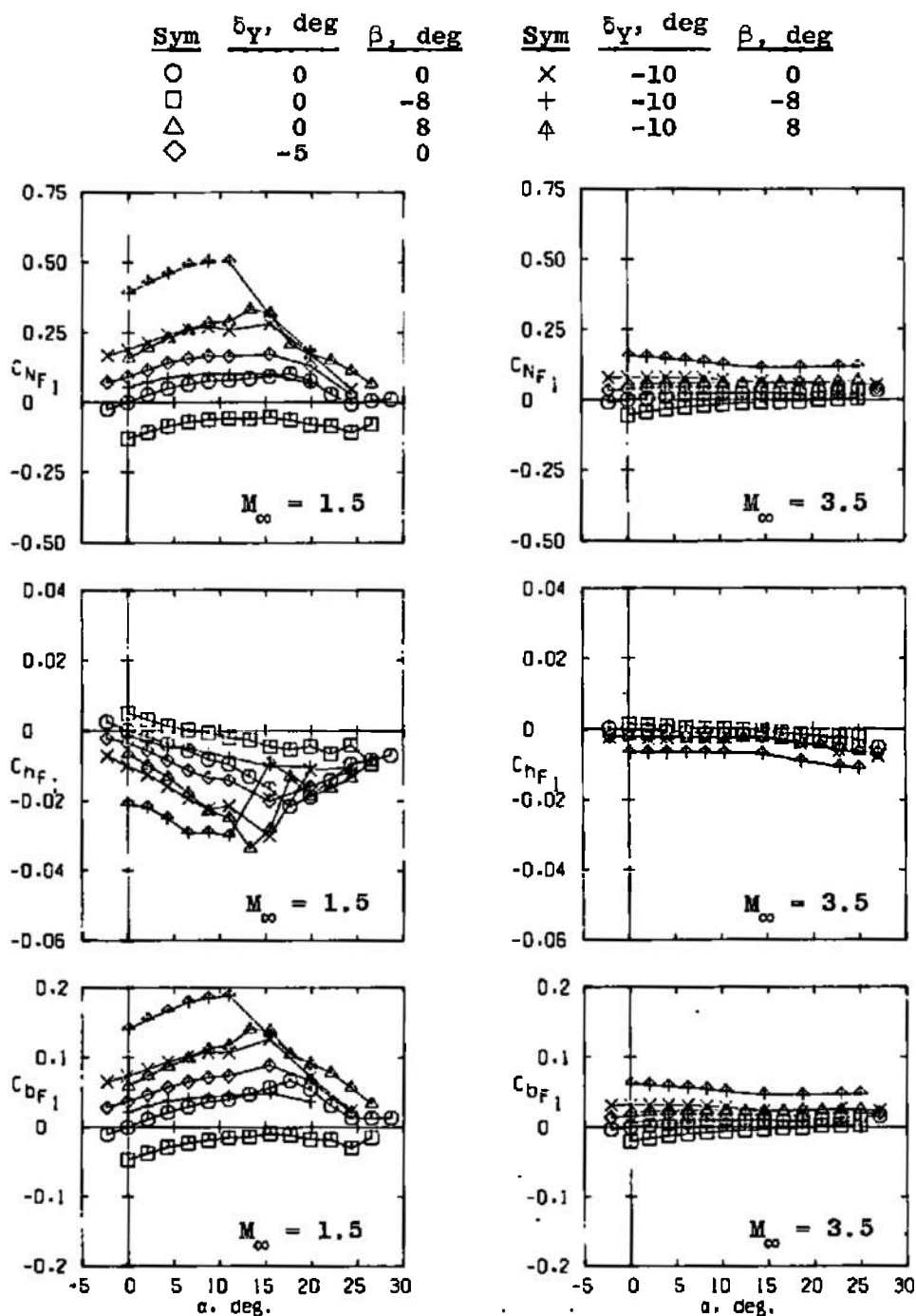
DECLASSIFIED / UNCLASSIFIED



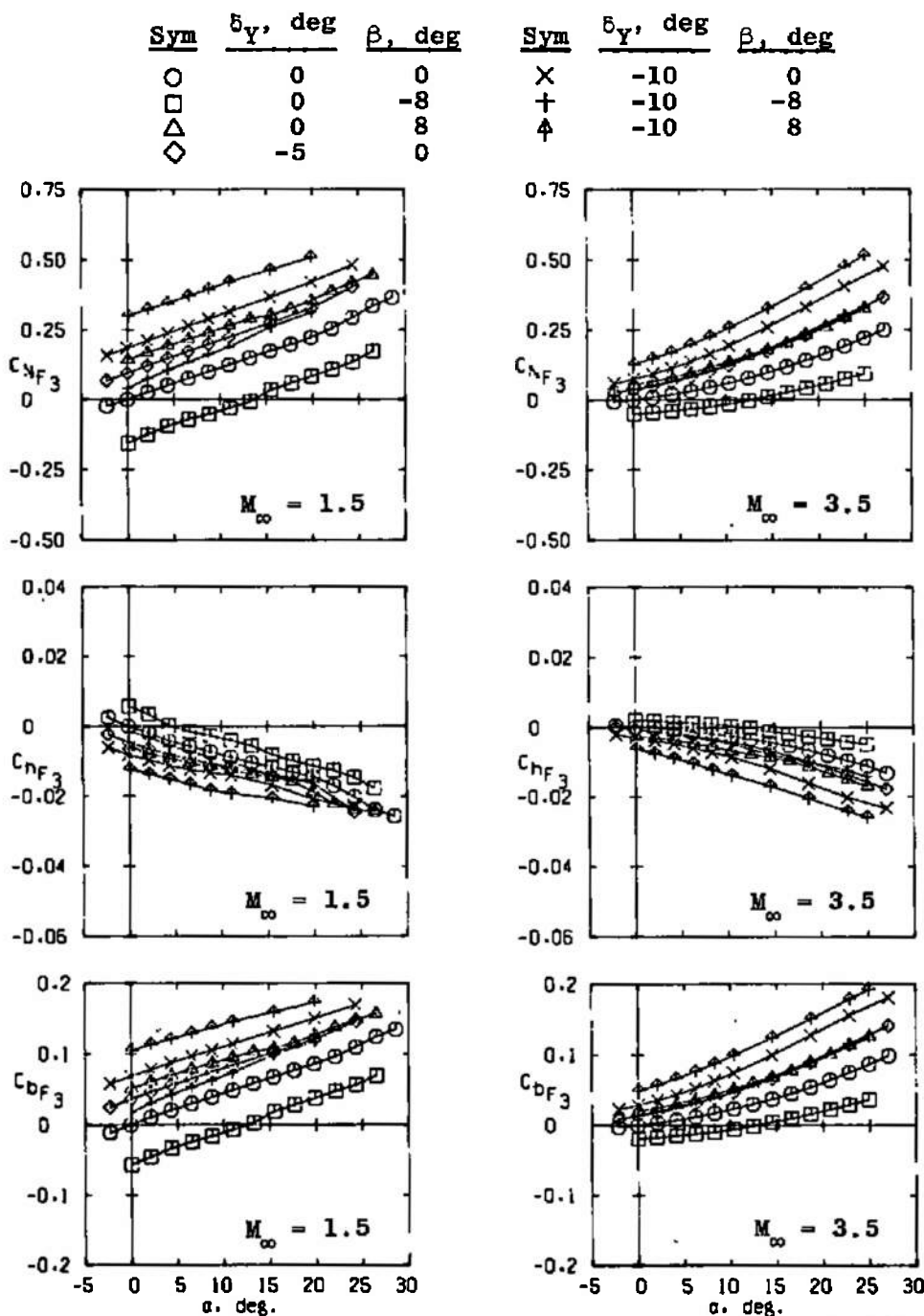
b. Missile axial force
Figure 9. Continued.

DECLASSIFIED / UNCLASSIFIED

CONFIDENTIAL



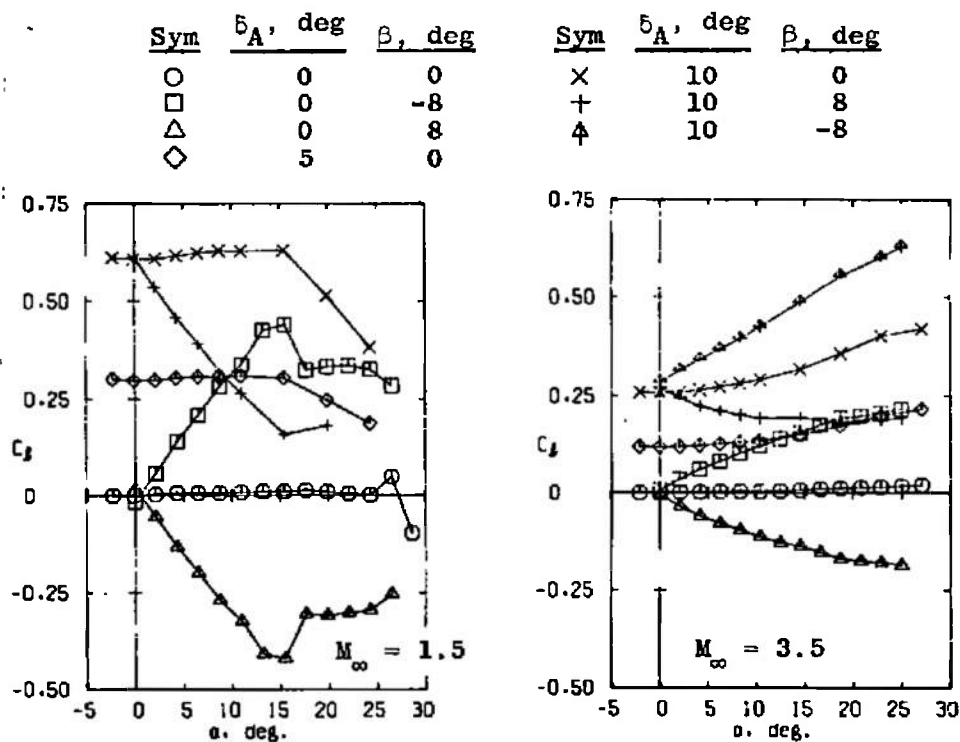
c. Fin 1 aerodynamic coefficients
Figure 9. Continued.

~~CONFIDENTIAL~~

d. Fin 3 aerodynamic coefficients
Figure 9. Concluded.

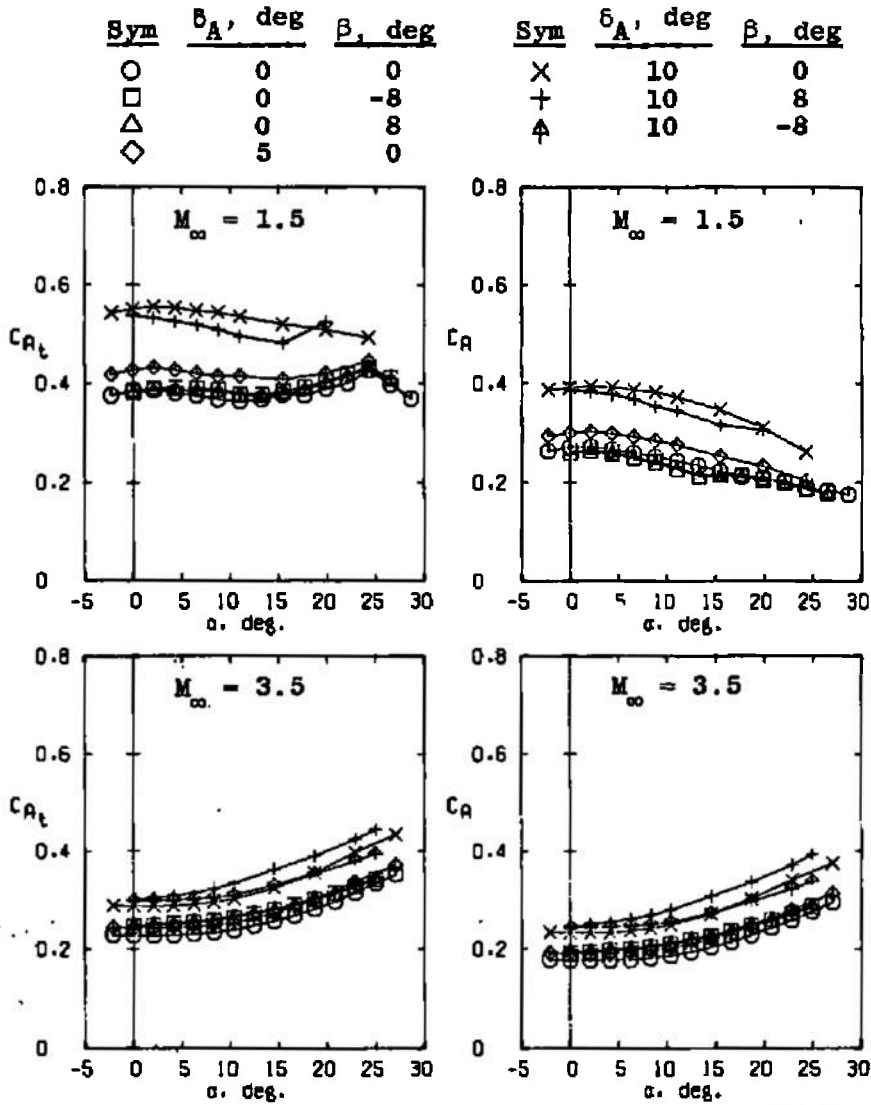
~~CONFIDENTIAL~~

DECLASSIFIED / UNCLASSIFIED

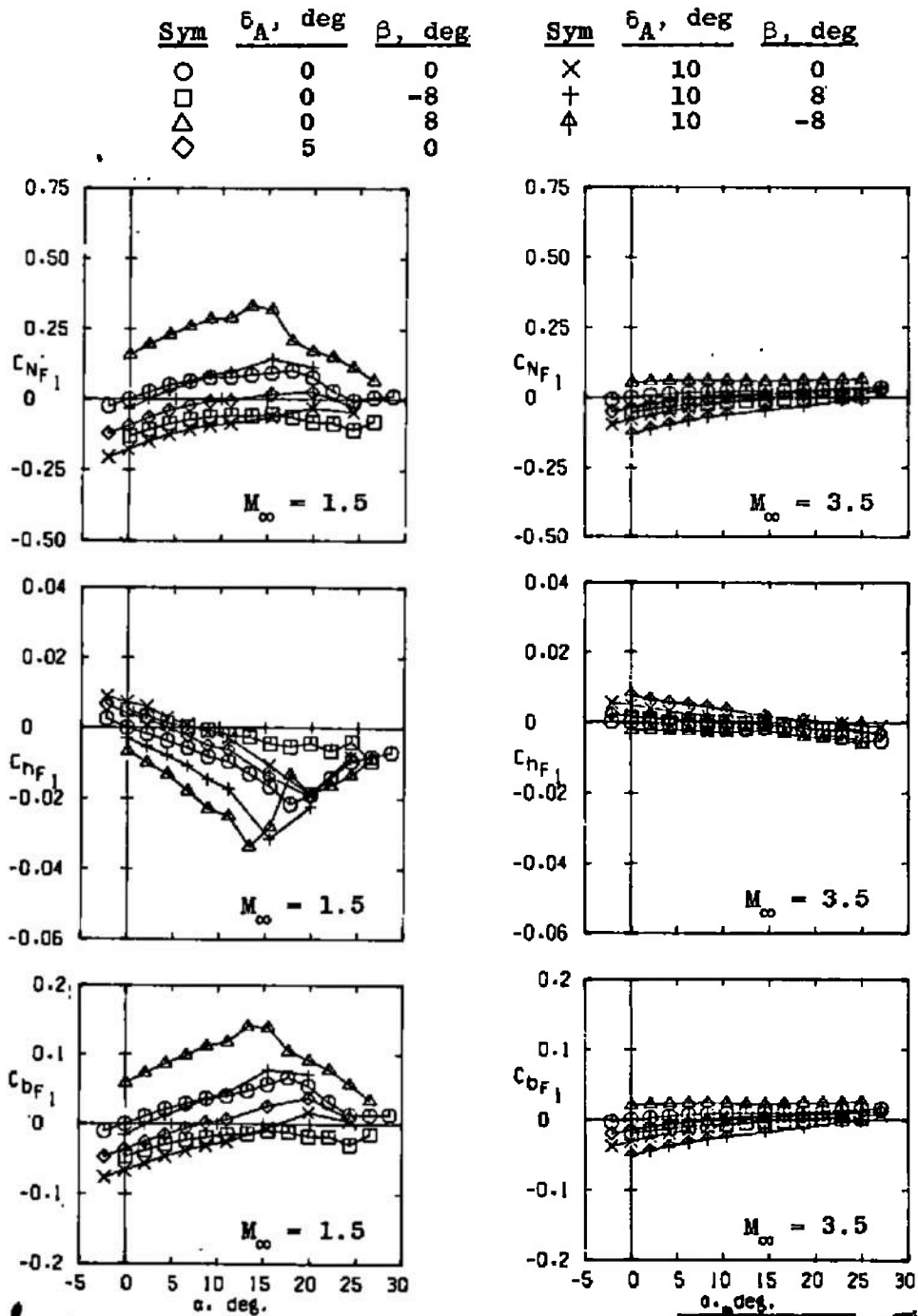


a. Rolling moment
Figure 10. Roll control characteristics.

DECLASSIFIED / UNCLASSIFIED

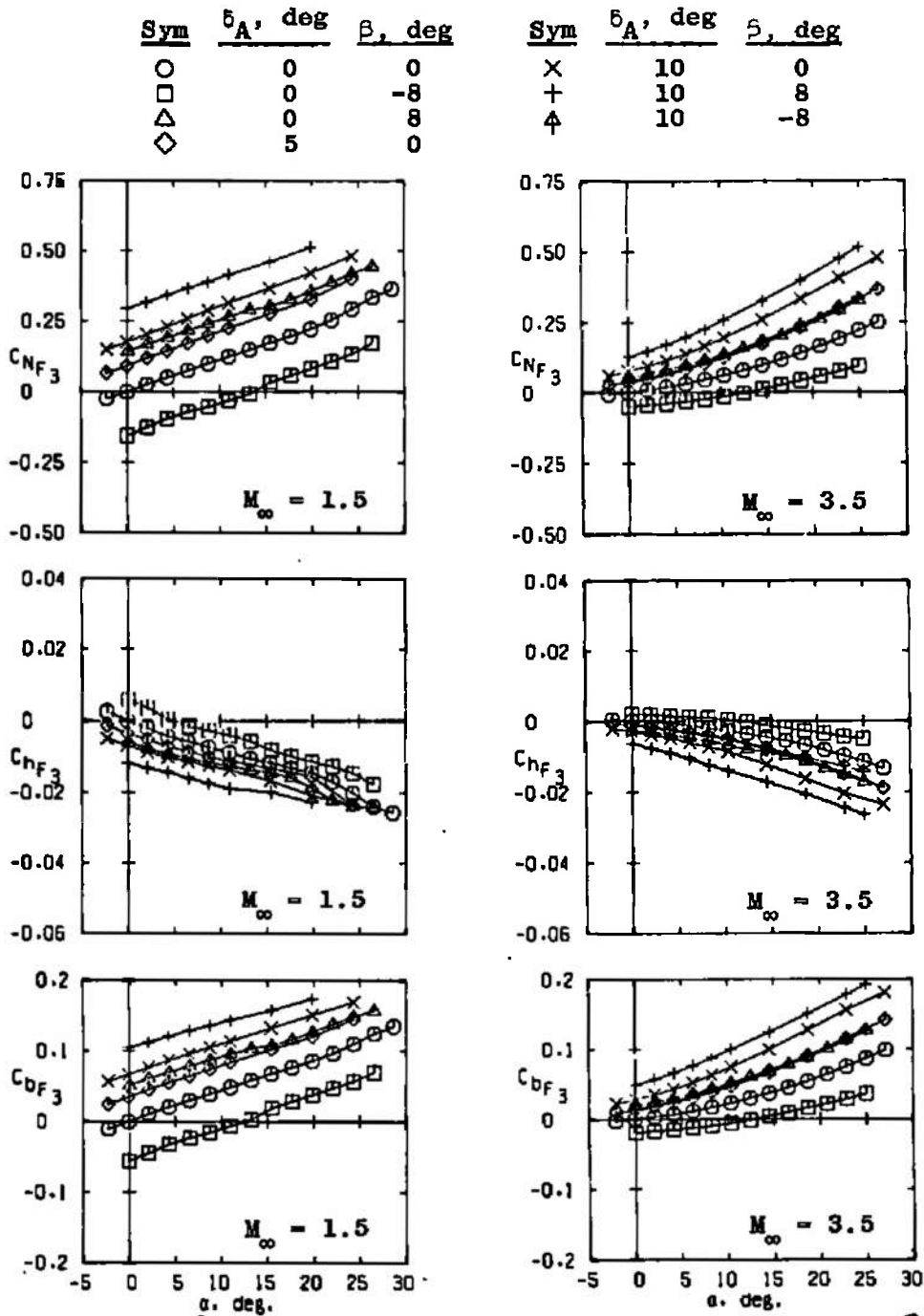


b. Axial force
Figure 10. Continued.



c. Fin 1 aerodynamic coefficients
Figure 10. Continued.

DECLASSIFIED / UNCLASSIFIED



d. Fin 3 aerodynamic coefficients
Figure 10. Concluded.

DECLASSIFIED / UNCLASSIFIED

Table 1. Test Summary

Fin Deflection, deg (see Fig. 4)			Mach Number														
			1.51					2.50					3.51				
			Sideslip angle (β), deg														
DEL-A, deg	DEL-P, deg	DEL-Y, deg	-8	-4	0	4	8	-8	-4	0	4	8	-8	-4	0	4	8
0	0	0	x	x	x	x	x	x	x	x	x	x	x	x	x	x	x
					x*					x*					x*		
5	0	0	x	x	x	x	x	x	x	x	x	x	x	x	x	x	x
10	0	0	x	x	x	x	x	x	x	x	x	x	x	x	x	x	x
0	-5	0	x	x	x	x	x	x	x	x	x	x	x	x	x	x	x
0	-10	0	x	x	x	x	x	x	x	x	x	x	x	x	x	x	x
0	-15	0	x	x	x	x	x	x	x	x	x	x	x	x	x	x	x
0	0	-5	x	x	x	x	x	x	x	x	x	x	x	x	x	x	x
0	0	-10	x	x	x	x	x	x	x	x	x	x	x	x	x	x	x
0	-10	-5			x					x							
5	-10	0			x					x							
5	-5	-5			x					x							
5	-5	0			x					x					x		
0	-5	-5			x					x							
5	0	-5			x					x					x		
5	-10	-5			x					x					x		
1.25	-8.75	1.25						x	x	x	x	x					
1.25	1.25	-8.75						x	x	x	x	x					

NOTES:

1. Asterisk (*) indicates model rolled 180 deg
2. Angle of attack ranges from -2 to 28 deg
3. $Re_m = 4.25$ million
4. Configuration BWF (body, -6 wings, -8 fins) for all groups
5. Fin deflection nomenclature redefined from tabulated data for compatibility with Ref. 1

UNCLASSIFIED

NOMENCLATURE

C_A	Model forebody axial-force coefficient, $C_{A_t} - C_{A_b}$
C_{A_b}	Model base axial-force coefficient, $-(P_b - p_\infty)/q_\infty$
C_{A_t}	Model total axial-force coefficient, total axial force/ $q_\infty S$
C_{b_F}	Fin root-bending moment coefficient, root-bending moment/ $q_\infty S l$ (about hinge line, Fig. 3c)
C_{h_F}	Fin hinge-moment coefficient, hinge moment/ $q_\infty S l$ (about hinge line, Fig. 3c)
C_ℓ	Model rolling-moment coefficient, rolling moment/ $q_\infty S l$
C_m	Model pitching-moment coefficient, pitching moment/ $q_\infty S l$ (see Fig. 3a for model cg)
C_N	Model normal-force coefficient, normal force/ $q_\infty S$
C_{N_F}	Fin normal-force coefficient, fin normal force/ $q_\infty S$
C_n	Model yawing-moment coefficient, yawing moment/ $q_\infty S l$ (see Fig. 3a for model cg)
C_Y	Model side-force coefficient, side force/ $q_\infty S$
$DEL-A, \delta_A$	Roll command deflection, deg (see Fig. 4)
$DEL-P, \delta_P$	Pitch command deflection, deg (see Fig. 4)
$DEL-Y, \delta_Y$	Yaw command deflection, deg (see Fig. 4)

l Moment reference length, 4.2363 in.

l_m Model length, 18.900 in.

M_∞ Free-stream Mach number

MS Model station, in.

p_b Model base pressure, psia

P_o Tunnel stilling chamber pressure, psia

P_∞ Free-stream static pressure, psia

q_∞ Free-stream dynamic pressure, psia

Re_{l_m} Free-stream Reynolds number based on model length

S Model reference area, 14.095 in.²

T_o Tunnel stilling chamber temperature, °R

α Model angle of attack, deg

β Model angle of sideslip, deg

SUBSCRIPTS

1 Fin 1 (see Figs. 3, 4, and 5)

3 Fin 3